

# Chordin and noggin promote organizing centers of forebrain development in the mouse

Ryan M. Anderson<sup>1</sup>, Alison R. Lawrence<sup>1</sup>, Rolf W. Stottmann<sup>1</sup>, Daniel Bachiller<sup>2</sup> and John Klingensmith<sup>1,\*</sup>

<sup>1</sup>Department of Cell Biology, Duke University Medical Center, Durham, NC 27710-3709, USA

<sup>2</sup>Victor Goodhill Ear Center, Head and Neck Surgery Division, University of California, Los Angeles, CA 90095-1794, USA

\*Author for correspondence (e-mail: kling@cellbio.duke.edu)

Accepted 23 July 2002

## SUMMARY

In this study we investigate the roles of the organizer factors chordin and noggin, which are dedicated antagonists of the bone morphogenetic proteins (BMPs), in formation of the mammalian head. The mouse chordin and noggin genes (*Chrd* and *Nog*) are expressed in the organizer (the node) and its mesendodermal derivatives, including the prechordal plate, an organizing center for rostral development. They are also expressed at lower levels in and around the anterior neural ridge, another rostral organizing center. To elucidate roles of *Chrd* and *Nog* that are masked by the severe phenotype and early lethality of the double null, we have characterized embryos of the genotype *Chrd*<sup>-/-</sup>;*Nog*<sup>+/-</sup>. These animals display partially penetrant neonatal lethality, with defects restricted to the head. The variable phenotypes include cyclopia, holoprosencephaly, and rostral truncations of the brain and craniofacial skeleton. In situ hybridization reveals a loss of SHH expression and signaling by the prechordal plate, and a decrease in FGF8 expression and signaling by the anterior neural ridge at the five-somite stage. Defective *Chrd*<sup>-/-</sup>;*Nog*<sup>+/-</sup> embryos exhibit reduced cell

proliferation in the rostral neuroepithelium at 10 somites, followed by increased cell death 1 day later. Because these phenotypes result from reduced levels of BMP antagonists, we hypothesized that they are due to increased BMP activity. Ectopic application of BMP2 to wild-type cephalic explants results in decreased FGF8 and SHH expression in rostral tissue, suggesting that the decreased expression of FGF8 and SHH observed in vivo is due to ectopic BMP activity. Cephalic explants isolated from *Chrd*;*Nog* double mutant embryos show an increased sensitivity to ectopic BMP protein, further supporting the hypothesis that these mutants are deficient in BMP antagonism. These results indicate that the BMP antagonists chordin and noggin promote the inductive and trophic activities of rostral organizing centers in early development of the mammalian head.

Key words: Chordin, Noggin, BMP, Holoprosencephaly, Prechordal plate, Forebrain, Mouse

## INTRODUCTION

The vertebrate gastrula organizer has been associated with early head development since the 1930s (Saxen, 1989). The mammalian organizer, the node, promotes anterior gene expression and is required for normal development of the head primordia (Ang and Rossant, 1994; Klingensmith et al., 1999). During the initial phases of vertebrate head development, regional organizing centers generate discrete subdivisions within the anterior neural plate. One of these organizing centers, the prechordal plate (PrCP), is a mesendodermal derivative of the node (Sulik et al., 1994). The PrCP is the rostral extreme of the axial mesendoderm and underlies the rostral-most midline of the neural plate; it confers dorsoventral pattern to overlying tissue via secreted molecules such as sonic hedgehog (SHH) (Pera and Kessel, 1997; Chiang et al., 1996; Shimamura and Rubenstein, 1997). Two other rostral organizers are the anterior neural ridge (ANR) and the isthmus organizer (IO). These generate pattern from within the

plane of the neural ectoderm. The ANR induces and promotes forebrain character, while the IO patterns neural tissue adjacent to the midbrain/hindbrain boundary (Rubenstein and Beachy, 1998). Both of these organizing centers express diffusible factors, including FGF8 (Crossley and Martin, 1995). Surgical and genetic ablation of the PrCP, ANR, IO or their effector molecules results in mispatterning and hypoplasia of the developing forebrain (Chiang et al., 1996; Houart et al., 1998; Meyers et al., 1998; Pera and Kessel, 1997; Schier et al., 1997).

BMPs also play important roles in development of the brain. Several BMPs are expressed in the mouse dorsal forebrain and facial primordia (Barlow and Francis-West, 1997; Furuta et al., 1997). Ectopic application of BMP4 to the ventral forebrain leads to holoprosencephaly in chick (Golden et al., 1999) and reduces expression of both *Shh* and *Fgf8* (Ohkubo et al., 2002). BMP4 applied to mouse forebrain explants represses anterior neural gene expression and may promote apoptosis in forebrain, hindbrain and craniofacial

neural crest (Furuta et al., 1997; Graham et al., 1994; Graham et al., 1996). These observations suggest that rostral tissues require proper control of BMP activity for normal development.

The distribution and activity of BMPs in the extracellular space is regulated by the secreted factors chordin (CHRD) and Noggin (NOG), which specifically bind BMP proteins and prevent ligation of their receptors (Sasai and De Robertis, 1997). The effects of both *Chrd* and *Nog* are mediated entirely by antagonism of BMP signaling, acting upstream of signal transduction (Hammerschmidt et al., 1996; Holley et al., 1995; Holley et al., 1996). Although similar biochemical activities suggest functional redundancy, CHRD and NOG display different binding affinities for various BMPs (Piccolo et al., 1996; Zimmerman et al., 1996) and interactions with extracellular modifiers (Ashe and Levine, 1999; Piccolo et al., 1997; Scott et al., 2001). Thus, CHRD and NOG may have both shared and specific roles.

Both *Chrd* and *Nog* are expressed in the node and its derivatives (Klingensmith et al., 1999; McMahon et al., 1998). Later in embryogenesis, they are expressed in diverse structures, some uniquely and others in common (Brunet et al., 1998; Scott et al., 2000). Null mutations for mouse *Chrd* and *Nog* have been generated to assess the role of these genes in mammalian development. *Chrd* null homozygotes are fully viable in outbred backgrounds with partially penetrant mild defects of the chondrocranium and cervical vertebrae (D. B. and J. K. unpublished). *Chrd* homozygosity, however, is lethal in inbred and defined hybrid backgrounds, resulting in severe chondrocranial and pharyngeal arch defects (Bachiller et al., 2000) (R. M. A., D. B., and J. K., unpublished). *Nog* null homozygotes die perinatally, with defects in dorsoventral patterning and skeletal development (McMahon et al., 1998; Brunet et al., 1998). Analysis of double null homozygotes reveals functional redundancy of *Chrd* and *Nog*. Regardless of genetic background, these embryos have severe forebrain truncations in addition to defects in dorsoventral and left-right patterning (Bachiller et al., 2000) (R. M. A. and J. K., unpublished).

In this study, we have examined a second class of *Chrd*;*Nog* double mutants, *Chrd*<sup>+/−</sup>;*Nog*<sup>+/−</sup>, to further elucidate the functions of these genes in head development. Our results indicate that *Chrd* and *Nog* promote growth and patterning signals from the PrCP and the ANR, two organizing centers of rostral development.

## MATERIALS AND METHODS

### Mice

*Chrd*<sup>RV</sup> heterozygotes (Bachiller et al., 2000) were bred to *Nog*<sup>9E</sup> heterozygotes (McMahon et al., 1998) to generate double heterozygous F<sub>1</sub> progeny. These were intercrossed to generate *Chrd*<sup>+/−</sup>;*Nog*<sup>+/−</sup> mice and were maintained on a random outbred ICR (Harlan) background. Mutant embryos were generated by timed matings of *Chrd*<sup>+/−</sup>;*Nog*<sup>+/−</sup> stock (Hogan et al., 1994). For comparative purposes, *Chrd*<sup>+/−</sup>;*Nog*<sup>+/−</sup> mice were generated and maintained in both 129Sv/J (Stottmann et al., 2001) and B6SJLF1 (Bachiller et al., 2000) genetic backgrounds. *Chrd*<sup>RV</sup> and *Nog*<sup>9E</sup> alleles were genotyped by PCR as described previously (Bachiller et al., 2000; McMahon et al., 1998). Embryos were staged as described previously (Downs and Davies, 1993; Kaufman, 1992).

### Gene expression assays

Whole-mount in situ hybridization was performed as already described (Belo et al., 1997). When necessary, staining buffer was supplemented with 5% polyvinyl alcohol (Aldrich #36, 313-8) to enhance weak signals. Standard techniques were used for β-galactosidase staining (Hogan et al., 1994). For RT-PCR, five-somite stage embryos were dissected into three pools of tissue using glass knives: trunk, ANR and anterior midline. The ANR region excluded rostromedial tissue to avoid potential ambiguity caused by expression in the midline mesendoderm. Preparation of cDNA samples and PCR for *Chrd* and *Hprt* were as described (Stottmann et al., 2001). *Nog* was detected using the following primers: 5'-GCATGGAGCG-CTGCCCCAGC and 5'-GAGCAGCGAGCGCAGCAGCG.

### Skeletal preparation and histological sectioning

Double staining of neonatal skeletons was performed as described (McLeod, 1980). For histological sectioning, embryos were fixed overnight in Bouin's fixative (histology) or 4% paraformaldehyde (TUNEL/immunohistochemistry), and washed in PBS before embedding in paraffin wax, sectioning (8 μm) and counterstaining according to standard protocols (Hogan et al., 1994).

### Cell death and proliferation

Nile Blue Sulfate (NBS) staining was performed as described (Trump et al., 1999), except embryos were incubated in Lactated Ringers containing 0.002% NBS (Sigma, N-5632) for 30 minutes at 37°C. Whole-mount TUNEL was performed as described (Conlon et al., 1995), except fragmented DNA was labeled with fluorescein-dUTP and detected with anti-fluorescein IgG (Roche). For apoptosis/proliferation assays, TUNEL was performed according to manufacturer's instructions using Fluorescein TUNEL labeling mix and TdT (Roche). Sections were then blocked in PBS containing 10% sheep serum, 1% blocking reagent (Roche) and 0.1% Tween-20 for 1 hour. Cells in metaphase were detected with anti-phosphorylated histone H3 IgG (Upstate Biotechnology) and an Alexa Red secondary antibody (Molecular Probes). Coverslips were mounted in 2.5% DABCO/90% glycerol.

At E8.5, proliferative and apoptotic indices were calculated by dividing number of metaphase-stage or TUNEL-positive cells by total number of DAPI-stained nuclei, respectively. At E9.5, indices were determined by dividing the number of labeled cells by total area of neural ectoderm. Area measurements were made using NIH image software. At least three adjacent sections were counted in each assay. Statistical significance assessed using Student's *t*-test.

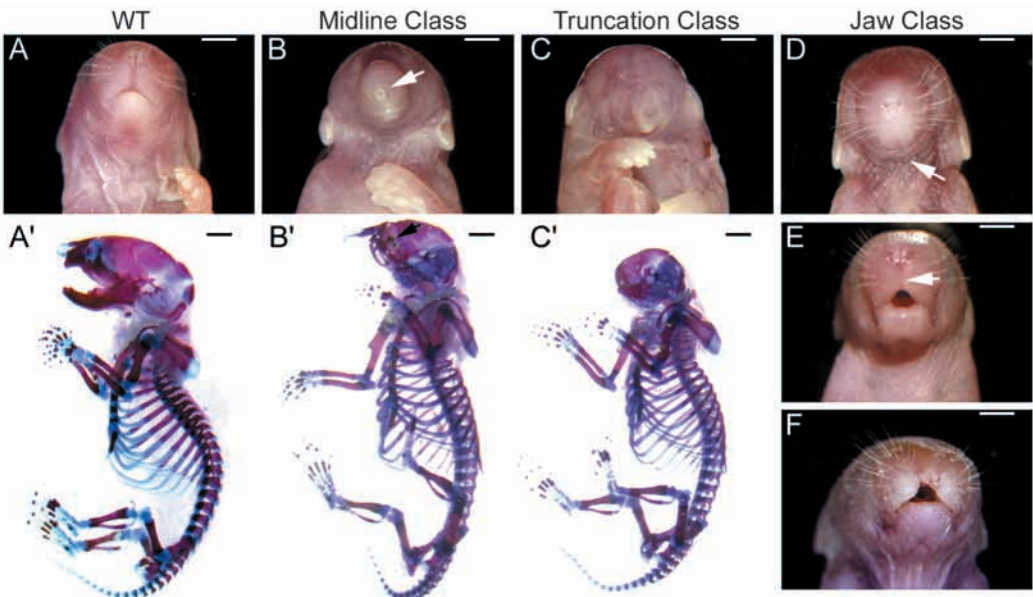
### Bead preparation and explant culture

Purified recombinant BMP2 (Genetics Institute) and BSA (Sigma) were applied to beads as described (Furuta et al., 1997). BMP2 was used at a concentration of 10 μg/ml unless otherwise indicated and BSA concentration was 1 mg/ml. Cephalic explants were isolated from five- to eight-somite embryos and contained all tissues rostral to the mid-hindbrain region. These were cultured on Nucleopore filters (Whatman) using media and culture conditions as described (Furuta et al., 1997).

## RESULTS

Double mutants bearing null alleles of *Chd* and *Nog* were constructed to address possible functional redundancy of these BMP antagonists in mammalian development. Two types of lethal *Chrd*;*Nog* double mutant phenotypes resulted. We observed an early lethal class with severe defects in each of the three primary embryonic axes, which corresponded to the double null genotype, *Chrd*<sup>+/−</sup>;*Nog*<sup>+/−</sup> (Bachiller et al., 2000). We also found a perinatally lethal group of cranial-restricted

**Fig. 1.** Spectrum of head defects in *Chrd*<sup>-/-</sup>;*Nog*<sup>+/-</sup> neonates. External anatomy of (A) wild type, (B) single nostril (arrow) with narrow proboscis, (C) anterior truncation, (D) agnathia (arrow) with two distinct nostrils, (E) mid-face hypoplasia with loss of philtrum (arrow) and (F) bilateral cleft lip. Skeletal preparations of animals are shown of A-C: (A') wild type, (B') cebocephaly with cyclopic eye (arrow) beneath proboscis and (C') anterior truncation. Skeletal structures caudal to the head are normal. Scale bar: 2 mm.



mutant phenotypes, which was comprised solely of the genotype *Chrd*<sup>-/-</sup>;*Nog*<sup>+/-</sup>. Rarely, *Chrd*<sup>-/-</sup>;*Nog*<sup>+/-</sup> animals with subtle craniofacial defects were viable. Conversely, some neonates died at birth with no overt defect. However, most animals of this genotype were viable and displayed no apparent defects. Remarkably, all phenotypes are restricted to the head with no defects discernable caudal to the neck (Fig. 1). The spectrum of phenotypes reflects a syndrome of neural and craniofacial malformations collectively known as holoprosencephaly (see below). By examining the basis of these rostral defects we have investigated the roles of *Chrd* and *Nog* in head development.

***Chrd*<sup>-/-</sup>;*Nog*<sup>+/-</sup> mice display three types of craniofacial skeletal defects**

Cranial development in *Chrd*<sup>-/-</sup>;*Nog*<sup>+/-</sup> animals ranges from outwardly normal to nearly headless. Three classes of defects may be distinguished among affected mutants, defined here as midline, truncation and jaw classes. The midline class shows absence of rostroventral midline structures often resulting in cyclopia (Fig. 1B,B', see Fig. 4P). The truncation class shows an absence of rostral-most tissues (Fig. 1C,C'). The jaw class lacks jaw elements derived from the first branchial arch and frontonasal mass (Fig. 1D-F). Although these defects are not mutually exclusive, one type usually predominates (Table 1).

**Table 1. Variation in *Chrd*<sup>-/-</sup>;*Nog*<sup>+/-</sup> neonatal defects**

Phenotypic group	Relative frequency
<b>Midline class</b>	<b>14 (53%)</b>
Single nostril	9 (35%)
Proboscis and synophthalmia/cyclopia	4 (15%)
Cleft palate	1 (4%)
<b>Truncation class</b>	<b>4 (15%)</b>
<b>Jaw class</b>	<b>8 (31%)</b>

Frequency of rostral phenotypes calculated from a subset of 26 affected *Chrd*;*Nog* neonates from consecutive outbred litters. Mutant pups containing more than one type of defect were classified according to the most severe defect.

In this study, we present our analysis of the initial neural defects in these mutants. Some mandibular phenotypes result from independent roles of *Chrd* and *Nog* in the first branchial arch (Stottmann et al., 2001). A study of the nature and causes of other defects in the craniofacial skeleton will be presented elsewhere (R. M. A., R. W. S. and J. K., unpublished).

**Anterior neural defects**

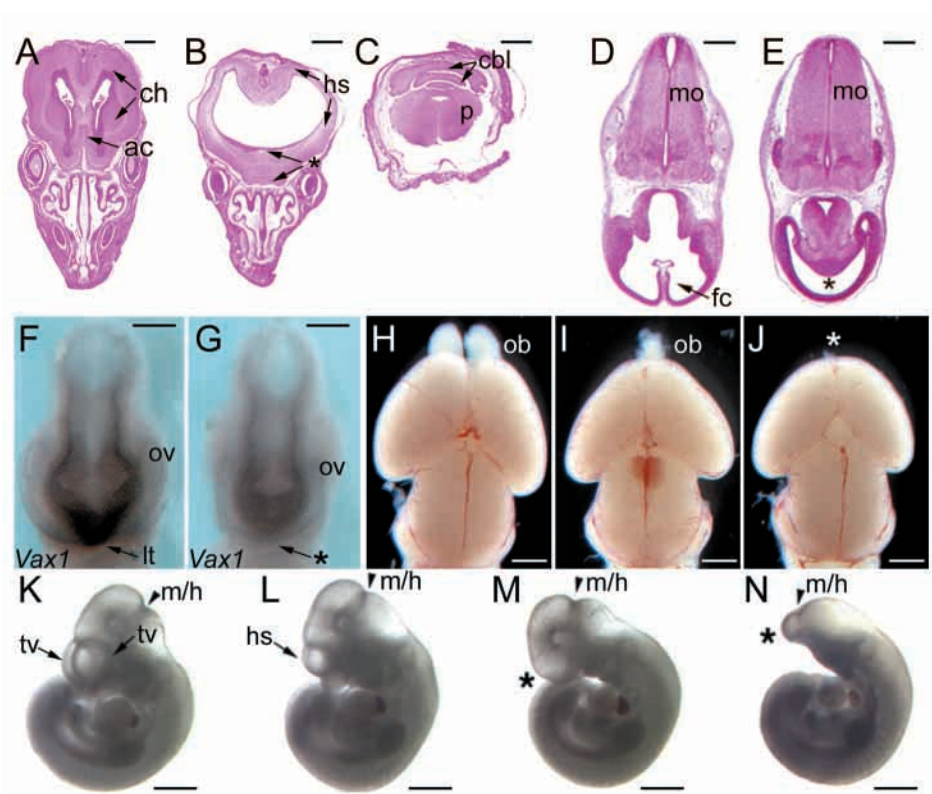
Holoprosencephaly (HPE) is a deficit of ventral midline development in the forebrain. In its most severe form, a holosphere is generated: a thin-walled, singly lobed cerebral structure with a common ventricle. Less severe forms and microforms also exist with less dramatic midline deletions. HPE is frequently associated with midline craniofacial defects in humans (Ming and Muenke, 1998). Affected *Chrd*<sup>-/-</sup>;*Nog*<sup>+/-</sup> mice exhibit a spectrum of HPE phenotypes observed throughout gestation (Fig. 2B,E,L). Significantly, loss of medial forebrain tissue is evident before evagination of the telencephalic vesicles, the precursors to the cerebral hemispheres (Fig. 2G). In the most severe cases, HPE is evident prior to neurulation (see Fig. 4M). Truncation class mutants that lack most of the facial skeleton also entirely lack rostral brain structures. Some severely affected animals lack forebrain and midbrain (Fig. 2C,N), while more modestly affected truncation mutants lack only the forebrain (Fig. 2M). In the mildest examples, mutants have fused or absent olfactory bulbs (Fig. 2I,J). Generally, mutant neural phenotypes correlate closely with external craniofacial defects.

**Penetrance of rostral defects in *Chrd*<sup>-/-</sup>;*Nog*<sup>+/-</sup> animals**

To reveal gestational lethality and penetrance of phenotypes in *Chrd*;*Nog* mutants, we assessed embryo development during early and late gestation. Prenatal lethality is apparent only in the double homozygote (Table 2), and presence of rostral-restricted phenotypes was perfectly correlated with the genotype *Chrd*<sup>-/-</sup>;*Nog*<sup>+/-</sup>. Overall, HPE phenotypes were observed in 9.0% of embryos examined from E8.5-17.5 and were first detectable at the five-somite stage (~E8.0).



**Fig. 2.** Midline and rostral neural defects. (A–C) Neonate transverse sections. (A) Wild type showing anterior commissure (ac) and bilateral cerebral hemispheres (ch). (B) Midline mutant lacking anterior commissure (asterisk) and showing cerebral hemispheres fused into a holosphere (hs). (C) Truncation mutant lacking CNS rostral to hindbrain. (D,E) E13.5 transverse sections. (D) Wild type showing medial falx cerebri (fc). (E) Midline mutant shows a single rostral ventricle (asterisk). (F,G) E9.5 embryos. (F) Wild-type embryo shows lamina terminalis (lt) marked by *Vax1* expression. (G) Midline mutant lacks lamina terminalis (asterisk). (H–J) Neonatal brains. (H) Wild type showing olfactory bulbs (ob). (I,J) Mild truncation mutant showing hypoplastic, fused olfactory bulbs (I) or lacking olfactory bulbs (J). (K,L) E10.5 embryos. (K) Wild type showing telencephalic vesicles (tv). (L) Midline mutant has single holospheric vesicle (hs). (M) Moderate truncation mutant lacks telencephalon (asterisk). (N) Severe truncation mutant lacks both forebrain and midbrain. mo, medulla oblongata; ov, optic vesicle; p, pons; cbl, cerebellum; m/h, midbrain/hindbrain boundary. Scale bars: 2 mm in A–C; 0.5 mm in D,E; 0.2 mm in F,G; 1 mm in H–N.



Furthermore, *Chrd*<sup>−/−</sup>;*Nog*<sup>+/-</sup> animals were under-represented by nearly 12% at weaning. This number reflects that in addition to the 9% of animals with overt HPE phenotypes, a further 3% of this mutant class die soon after birth with few, if any, detectable external defects. For example, most juvenile *Chrd*<sup>−/−</sup>;*Nog*<sup>+/-</sup> mice were externally normal, but some had mild midline defects such as an absence of upper incisors (*n*=4; data not shown).

Haploinsufficiency of *Nog* for forebrain development occurs only in the absence of *Chrd* (Table 3). However, the penetrance of these defects is low in a random-outbred genetic background. One theoretical explanation for this is that other potential genetic modifiers influence *Chrd* and *Nog* function in the midline. Indeed, the mutant phenotypes observed in *Chrd*<sup>−/−</sup> mice differ significantly with genetic background (see Introduction). Because of this sensitivity, we tested whether

*Chrd*<sup>−/−</sup>;*Nog*<sup>+/-</sup> animals might have full penetrance of rostral phenotypes in defined genetic backgrounds. However, we found that most *Chrd*<sup>−/−</sup>;*Nog*<sup>+/-</sup> pups of both inbred (129Sv/J) and hybrid (B6SJL/F1) strains exhibited no discernible holoprosencephalic phenotypes and were fully viable (Table 3, data not shown). Given the low fecundity of inbred mice and no evidence for increased phenotypic penetrance, we conducted all subsequent studies in an outbred genetic background.

**Expression of *Chordin*, *Noggin* and BMPs during early neural patterning**

To understand more fully the functions of *Chrd* and *Nog* in head formation, we characterized their expression from neural plate through early organogenesis stages (~E7.5–8.5). The prechordal plate (PrCP) is identifiable by the co-expression of *Gsc*, *Shh* and *Foxa2* (Fig. 3B–D) (Belo et al., 1998; Camus et al., 2000). In situ hybridization at headfold and early somite

**Table 2. Frequency of genotypic and phenotypic classes**

Age	<i>Chrd</i> <sup>−/−</sup> ; <i>Nog</i> <sup>+/+</sup>	<i>Chrd</i> <sup>−/−</sup> ; <i>Nog</i> <sup>+/-</sup>	<i>Chrd</i> <sup>−/−</sup> ; <i>Nog</i> <sup>−/−</sup>	Number of rostral phenotypes in <i>Chrd</i> <sup>−/−</sup> ; <i>Nog</i> <sup>+/-</sup>
E7.5	30 (29.4%)	50 (49%)	22 (21.6%)	0
E8.5	66 (29%)	116 (51%)	46 (20%)	9 (8%)
E9.5	40 (27%)	80 (55%)	26 (18%)	8 (10%)
E17.5	24 (38%)	38 (60%)	1 (1.6%)	4 (11%)
P28	67 (40%)	96 (60%)	0	0

These data represent only a subset of total embryos examined. Double null phenotypes were essentially as described (Bachiller et al., 2000). All rostral-restricted phenotypes genotyped as *Chrd*<sup>−/−</sup>;*Nog*<sup>+/-</sup>. Penetrance was calculated as the percentage of *Chrd*<sup>−/−</sup>;*Nog*<sup>+/-</sup> animals with phenotypes. At weaning, *Chrd*<sup>−/−</sup>;*Nog*<sup>+/-</sup> mice were under-represented by 11.7% (*P*=0.035).

**Table 3. Frequency of rostral deletion phenotypes in different genetic backgrounds**

Strain	<i>Chrd</i> <sup>−/−</sup> ; <i>Nog</i> <sup>+/+</sup>	<i>Chrd</i> <sup>+/-</sup> ; <i>Nog</i> <sup>+/-</sup>	<i>Chrd</i> <sup>−/−</sup> ; <i>Nog</i> <sup>+/-</sup>	<i>Chrd</i> <sup>−/−</sup> ; <i>Nog</i> <sup>−/−</sup>
129SVJ (inbred)	1.8%; <i>n</i> =57	0%; <i>n</i> =127	0%; <i>n</i> =5*	n/a*
B6SJL/F1 (hybrid)	0%; <i>n</i> >100	0%; <i>n</i> >100	4.5%; <i>n</i> =22	100%†
ICR (outbred)	0%; <i>n</i> >403	0%; <i>n</i> >174	9.0%; <i>n</i> =234	100%; <i>n</i> >73

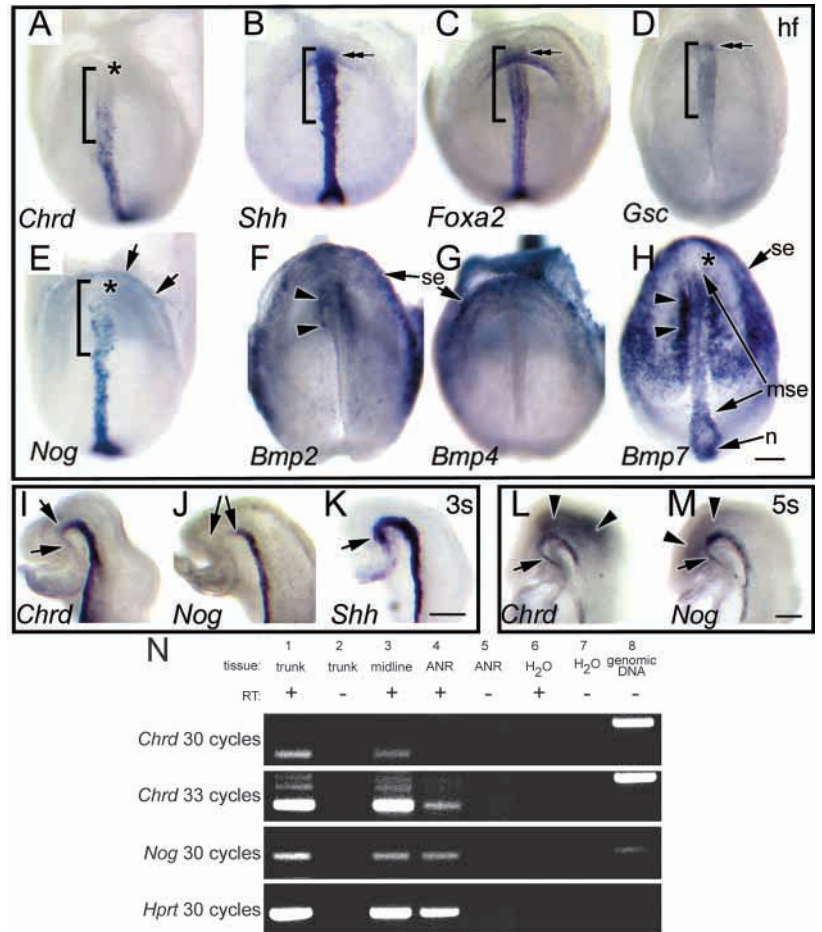
Embryos of each genotype were examined for rostral midline or truncation phenotypes between the ages of E9.5 and P28.  
\*Low fecundity in 129 background prevented detailed study of double mutants.  
†Bachiller et al., 2000.  
n/a, not applicable.

stages reveals axial expression of *Chrd* and *Nog* through the caudal PrCP; neither is expressed in the rostral PrCP at these stages (Fig. 3A,E,I,J). Thus, the initial limit of *Chrd* and *Nog* expression defines rostral and caudal subregions within the PrCP. By the five-somite stage, however, *Chrd* and *Nog* are expressed throughout the axial mesendoderm, including the PrCP (Fig. 3L,M). *Chrd* and *Nog* are also clearly expressed in cephalic mesenchyme (Fig. 3L,M), and *Nog* is expressed near the anterior neural ridge (ANR), the boundary between surface and neural ectoderm (Fig. 3E). We did not detect *Chrd* in the ANR by in situ analysis; however, RT-PCR amplification demonstrates a low level of *Chrd* expression in the non-midline ANR, at early somite stages (Fig. 3N). In summary, *Chrd* and *Nog* are both expressed in the axial mesendoderm including the PrCP, although expression in the rostral-most PrCP is delayed until the five-somite stage. They are also expressed in or around the ANR. Thus, both genes are expressed in two of the known organizing centers of rostral head development.

Because CHRD and NOG presumably influence BMP signaling only where target BMPs are present (Piccolo et al., 1996; Zimmerman et al., 1996), we examined expression of BMP2, BMP4 and BMP7 at headfold through early somite stages (Fig. 3F-H). Each is expressed in epidermis adjacent to the neural plate. Furthermore, *Bmp2* and *Bmp7* are expressed in paraxial mesoderm adjacent to axial mesendoderm. *Bmp7* is co-expressed with *Chrd* and *Nog* in the node, notochord and caudal PrCP. Collectively, several relevant BMPs are expressed such that they may interact with CHRD and NOG, and influence PrCP and ANR activities.

### Rostral defects involve loss of SHH signaling

Defects in *Chrd*<sup>-/-</sup>; *Nog*<sup>+/-</sup> pups resemble rostral holoprosencephaly phenotypes seen in *Shh*<sup>-/-</sup> mice (Chiang et al., 1996). Furthermore, humans heterozygous for *SHH* display a range of phenotypes almost identical to that seen in *Chrd*<sup>-/-</sup>; *Nog*<sup>+/-</sup> mice (Roessler et al., 1996). We therefore examined *Shh* expression and signaling in *Chrd*<sup>-/-</sup>; *Nog*<sup>+/-</sup> mutants. In affected embryos, *Shh* expression is absent from the rostral mesendoderm and the rostral ventral neural midline (RVNM; Fig. 4A,B,E,F), while more caudal domains are unaffected. Patched 1 (*Ptch1*; *Ptch* – Mouse Genome Informatics) and *Gli1* are positively regulated transcriptional targets of SHH (Lee et al., 1997; Marigo and Tabin, 1996). Therefore, expression levels reflect SHH signal transduction. *Ptch1* and *Gli1* expression is diminished or lost in the RVNM of affected *Chrd*<sup>-/-</sup>; *Nog*<sup>+/-</sup> embryos (Fig. 4C,G; data not shown). SHH also induces the expression of *Nkx2.1* (*Titf1* – Mouse Genome Informatics) in the presumptive ventral diencephalon (Dale et al., 1997; Shimamura and Rubenstein, 1997), and this expression is critical for pituitary development



**Fig. 3.** Wild-type expression of *Chrd*, *Nog* and *Bmps*. (A-H) Frontal aspect of headfold stage (E7.75) embryos. Bracketed area represents approximate extent of *Gsc* expression, a prechordal plate (PrCP) marker. (A) *Chrd* is not expressed in the rostral-most PrCP (asterisk). (B) *Shh* and (C) *Foxa2* are expressed in all midline mesendoderm, including rostral PrCP (double arrows). (D) *Gsc* is expressed throughout the PrCP. (E) *Nog* is not expressed in the rostral PrCP (asterisk), but is expressed in the ANR (arrows). (F-H) BMPs antagonized by CHRD and NOG are expressed in surface ectoderm (se), rostral paraxial mesoderm (arrowheads), node (n) and midline mesendoderm (mse). *Bmp7* is not expressed in the rostral PrCP (H, asterisk). (I-K) Lateral aspect of bisected three-somite stage embryos. Neither *Chrd* (I) nor *Nog* (J) is detected in rostral PrCP at this stage by in situ hybridization, although *Shh* (K) is present (arrows). *Chrd* (L) and *Nog* (M) are both expressed throughout the rostral axial mesendoderm by the five-somite stage (arrows) and in head mesenchyme (arrowheads). Scale bar: 0.2 mm. (N) RT-PCR analysis of *Chrd* and *Nog* expression. *Chrd* and *Nog* are detected in the midline and trunk after 30 cycles of PCR (lanes 1,3). *Nog* is evident in the ANR (lane 4) after 30 cycles, and *Chrd* after additional amplification.

(Kimura et al., 1996; Takuma et al., 1998). *Nkx2.1* expression is lost in affected *Chrd*<sup>-/-</sup>; *Nog*<sup>+/-</sup> mutants (Fig. 4D,H), resulting in aberrant infundibulum development (Fig. 4L,P). Together, these results indicate that the most rostral expression of *Shh* is lost in affected *Chrd*<sup>-/-</sup>; *Nog*<sup>+/-</sup> embryos, with a consequential diminishment of SHH signaling and PrCP function.

### Loss of anterior FGF8 expression and signaling

A total lack of SHH results in holoprosencephaly but not truncation of rostral structures (Chiang et al., 1996). We therefore suspected that an additional defect in *Chrd*<sup>-/-</sup>; *Nog*<sup>+/-</sup>



**Fig. 4.** Loss of rostral SHH and FGF8 expression and signaling.

(A,B,E,F,K,O) Lateral aspect, (C,D,G,H) ventral aspect and (I,J,M,N) frontal aspect of cephalic region. Wild-type expression of *Shh* (A,B), *Ptch1* (C), *Nkx2.1* (D).

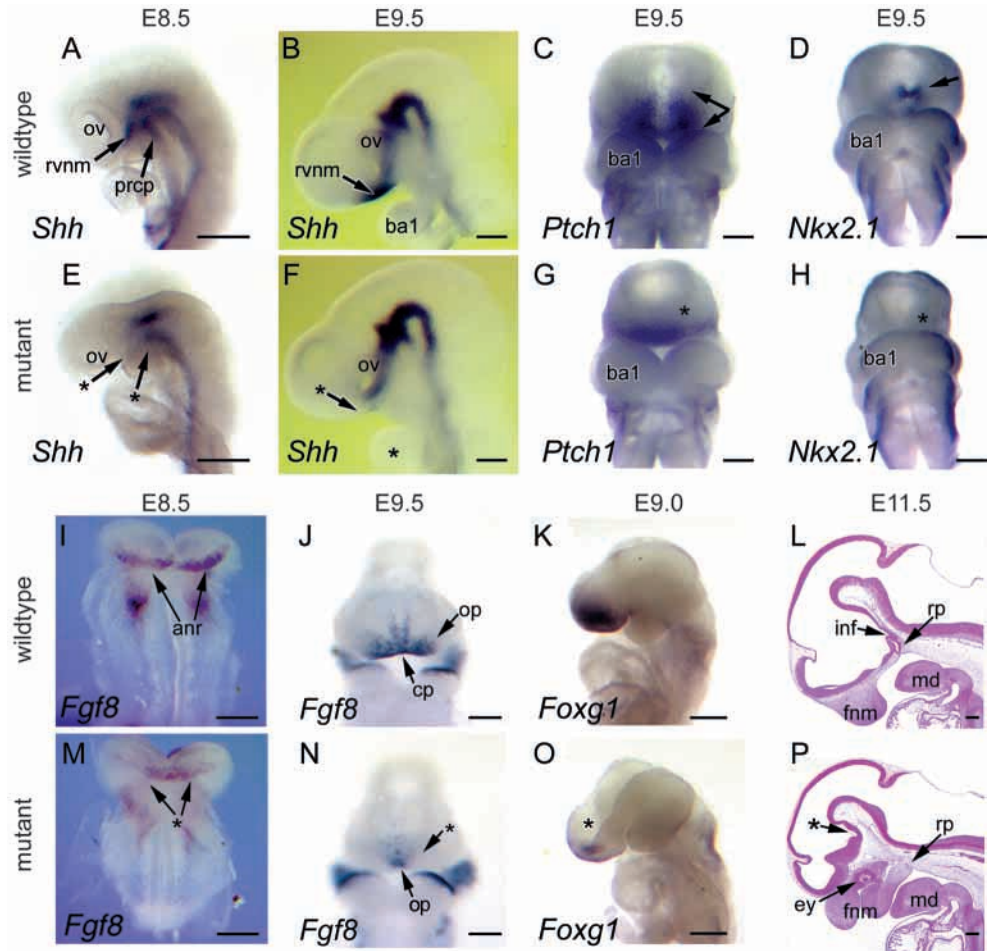
(E) E8.5 mutant (approx. eight to 10 somites) lacking *Shh* in RVNM and PrCP (asterisks;  $n=2$ ). (F) E9.5 (~20–25 somites) mutant lacking expression in RVNM (asterisk;  $n=5$ ).

Note loss of *Shh* expression in first branchial arch (lower asterisk, ba1 in B). (G) Midline mutant lacking rostral *Ptch1* expression (asterisk;  $n=4$ ). (H) Midline mutant lacking rostral *Nkx2.1* expression (asterisk;  $n=2$ ).

Wild-type expression of *Fgf8* (I,J) and *Foxg1* (formerly known as *BF-1*; K). (M) E8.25 (approx. five somites) mutant with diminished expression of *Fgf8* in the ANR which is confined to the midline (asterisk;  $n=2$ ). (N) E9.5 mutant with diminished *Fgf8* expression in the commissural plate and olfactory placodes (asterisk;  $n=4$ ). (O) Reduced *Foxg1* expression (asterisk) in E9.0 (~17 somites) mutant. (L,P) Mid-sagittal sections of E11.5 embryos.

(L) In wild type, infundibulum (inf) and Rathke's pouch (rp) interact to form mature pituitary. (P) In midline mutant, infundibulum does not develop (asterisk) and Rathke's pouch is rudimentary. Note cyclopic eye (ey).

anr, anterior neural ridge; prcp, prechordal plate; rvnm, rostral ventral neural midline; cp, commissural plate; op, olfactory placodes; fnm, frontonasal mass; md, mandible; ov, optic vesicle. Scale bar: 0.2 mm.



mice caused the rostral truncations. The ANR has an important role in patterning and growth of the rostral neural tube, which is mediated at least in part by FGF8 expression (Rubenstein and Beachy, 1998; Meyers et al., 1998; Shimamura and Rubenstein, 1997). We therefore examined expression of *Fgf8* and its downstream target *Foxg1* (Shimamura and Rubenstein, 1997) in affected *Chrd*<sup>-/-</sup>; *Nog*<sup>+/-</sup> embryos. At five somites (~E8.0), *Fgf8* is expressed in bilateral domains of the ANR (Fig. 4I). However, affected *Chrd*<sup>-/-</sup>; *Nog*<sup>+/-</sup> embryos have reduced expression of *Fgf8* in a single domain, fused at the midline (Fig. 4M). At E9.5, *Fgf8* is expressed in the commissural plate and lateral epithelial domains of developing nasal placodes (Crossley and Martin, 1995) (Fig. 4J). Moderately affected embryos retain only a medial domain of rostral *Fgf8* expression at dramatically reduced levels (Fig. 4N). Expression of *Foxg1* is correspondingly reduced in the prosencephalon (Fig. 4K,O). These data indicate that FGF8 expression and signaling are reduced in affected *Chrd*<sup>-/-</sup>; *Nog*<sup>+/-</sup> embryos.

The reduction of *Shh* and *Fgf8* expression and signaling that we have observed could be due to prior loss of cells expressing these genes. However, we have not detected morphological changes prior to the five-somite stage. Moreover, no *Chrd*<sup>-/-</sup>; *Nog*<sup>+/-</sup> embryos at late headfold stages showed evidence of increased apoptosis as measured by whole-mount

TUNEL assay ( $n=41$ ). Therefore we conclude that rostral neural ectoderm domains affected in *Chrd*<sup>-/-</sup>; *Nog*<sup>+/-</sup> embryos are initially present at the time *Shh* and *Fgf8* are normally first expressed. Moreover, the overall frequency of *Chrd*<sup>-/-</sup>; *Nog*<sup>+/-</sup> embryos displaying diminished *Shh* or *Fgf8* was similar to the penetrance of morphological phenotypes (not shown).

### Cell death and proliferation

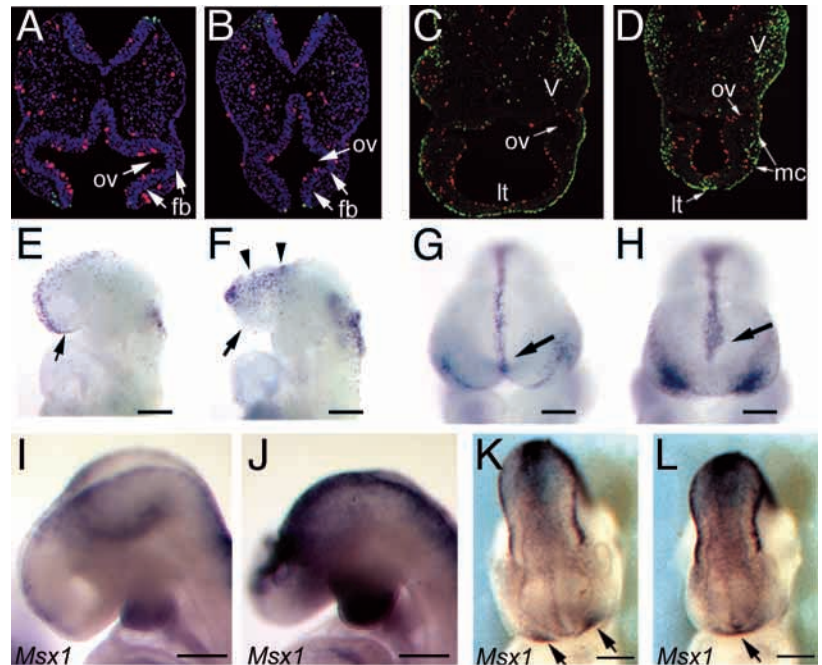
Many brain and craniofacial structures are clearly absent in affected *Chrd*<sup>-/-</sup>; *Nog*<sup>+/-</sup> embryos by organogenesis stages. We therefore used sectioned embryos to analyze levels of apoptosis via TUNEL reaction and proliferation via anti-phosphorylated histone H3 antibody staining. At eight to 10 somites (~E8.5), cell proliferation is greatly decreased in the forebrain of affected *Chrd*<sup>-/-</sup>; *Nog*<sup>+/-</sup> embryos, although apoptosis appeared comparable with wild type (Fig. 5A,B). By contrast, affected 20–25 somite (~E9.5) *Chrd*<sup>-/-</sup>; *Nog*<sup>+/-</sup> embryos displayed expansion of death in the dorsal midline, lateral head mesenchyme and the trigeminal ganglion, but normal levels of neural proliferation (Fig. 5C,D). As another measure of apoptosis, we stained whole embryos with Nile Blue sulfate (NBS), which marks non-necrotic cell death. NBS staining at eight to 10 somites reveals mildly increased dorsal staining not detected in sections (Fig. 5E,F). Unexpectedly, normal

ventromedial domains of apoptosis were absent, suggesting that tissues in this region have been deleted or mis-specified. At 20–25 somites, the dorsomedial stripe of NBS-positive cells was broadened in affected mutants (Fig. 5G,H). Again, the ventral midline domain of cell death was absent in affected embryos. Based on the timing of changes in gene expression relative to cell death increases elsewhere, we suspect that this loss of a normal domain of cell death is due to mis-specification of this tissue, rather than an early total deletion of the entire tissue. Collectively, these results indicate that cell proliferation is reduced in the forebrain at eight to 10 somites, following the first changes in rostral gene expression. Apoptosis levels may be mildly elevated at this stage. By 20–25 somites, proliferation levels have normalized in the forebrain, but cell death is dramatically increased in forebrain and surrounding tissues.

Apoptosis via BMP activity may be mediated by *Msx* transcription factors (Marazzi et al., 1997), and *Msx* transcription is positively regulated by BMP2 and BMP4 in the forebrain (Furuta et al., 1997). Moreover, *Msx1* may repress expression of anterior neural genes (Feledy et al., 1999). We have observed increased expression of *Msx1* in *Chrd<sup>-/-</sup>;Nog<sup>-/-</sup>* double homozygous embryos (R. M. A. and J. K., unpublished). In addition, more severely affected *Chrd<sup>-/-</sup>;Nog<sup>+/-</sup>* embryos may display robust increases in *Msx1* expression (Fig. 5I,J). However, there is no clear change in most moderately affected *Chrd<sup>-/-</sup>;Nog<sup>+/-</sup>* embryos (Fig. 5K,L), and spatial differences reflect only the absence of midline tissue. Thus, although we observe changes in apoptosis and proliferation in all affected *Chrd;Nog* mutants, only the more severe phenotypes also display a clear increase in *Msx1* expression. Therefore it is possible that *Msx1* induction is a transient response to BMP signaling in some contexts (see more below).

### An explant assay for addressing the consequences of increased BMP activity

Increased BMP signaling is anticipated with the loss of *Chrd* and *Nog*; thus, unantagonized BMP signaling probably causes the defects seen in *Chrd<sup>-/-</sup>;Nog<sup>+/-</sup>* embryos. To test the effects of locally increased BMP activity, we cultured cephalic explants from five- to eight-somite embryos in combination with beads soaked in recombinant BMP2. Explants were prepared by placing a single bead against the ANR between the bilateral anterior neural folds (designated type 1). To confirm the presence of increased BMP signaling, we examined the expression of the direct BMP target *Msx1* (Table 4, part A). *Msx1* was strongly induced in regions adjacent to BMP2 beads (Fig. 6A). Strikingly, *Msx1* was induced laterally at large distances (hundreds of  $\mu\text{m}$ ) from the bead, but did not extend into the midline of the explant. This suggests that BMPs may act at long range in the ANR, and that some regions of the head are refractory to *Msx1* induction by BMP signaling. We tested



**Fig. 5.** Analysis of apoptosis and cell proliferation in *Chrd<sup>-/-</sup>;Nog<sup>+/-</sup>* mutants. (A–D) TUNEL/proliferation assay on sections of wild-type (A,C) and *Chrd<sup>-/-</sup>;Nog<sup>+/-</sup>* mutant (B,D) embryos. E8.5 *Chrd<sup>-/-</sup>;Nog<sup>+/-</sup>* mutant (B) shows a 36% decrease in proliferation (labeled in red,  $P=0.018$ ), while differences in apoptosis (labeled in green) were not observed in section. E9.5 mutant (D) shows a nearly 10-fold increase in apoptotic cells (947%;  $P=0.019$ ) in the neural ectoderm rostral to the optic vesicles (ov). Increased apoptosis is also seen in rostral mesenchyme (mc) and trigeminal ganglion (V). Proliferation at E9.5 is not significantly different from wild type. Similar results were seen in three or more independent experiments. (E–H) Nile Blue Sulfate staining of wild-type (E,G) and *Chrd<sup>-/-</sup>;Nog<sup>+/-</sup>* mutant (F,H) embryos. (F) Lateral aspect of eight- to 10-somite mutant showing expansion of apoptosis in dorsal domains (arrowheads), and loss from the ventral midline (arrow;  $n=3$ ). (H) Frontal aspect of 20–25 somite mutant showing expanded apoptosis in the dorsal midline (arrows) and frontonasal mass ( $n=5$ ). (I–L) Rostral expression of *Msx1* in wild-type (I,K) and *Chrd<sup>-/-</sup>;Nog<sup>+/-</sup>* mutants (J,L). (J) In severely affected mutants, rostral domains of *Msx1* are expanded at eight to 10 somites ( $n=2$ ). At E9.5 *Chrd<sup>-/-</sup>;Nog<sup>+/-</sup>* expression domains have shifted toward the midline (L, arrow) though expression levels are comparable with those in wild type ( $n=3$ ). Scale bars: 0.2 mm.






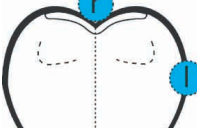
this by placing a BMP bead directly on the midline (designated type 2 explants). In these, the midline responded with *Msx1* induction, but not in the most rostral part (Fig. 6D). Ectopic BMP2 was probably present in this region, as *Msx1* induction was seen beyond this zone, in medial regions of the ANR.

Because we observed no clear increase in *Msx1* expression in some affected *Chrd<sup>-/-</sup>;Nog<sup>+/-</sup>* embryos, we suspected that increased *Msx1* expression may be a transient response to modestly increased BMP activity in these tissues. We used our explant assay to address the duration of *Msx1* expression as a response to exogenous BMP2. *Msx1* was strongly expressed in the ANR after 6 hours of culture with BMP beads (Fig. 6A). After 9 hours, expression was markedly diminished, and more so at 12 hours (Fig. 6B,C).

### BMP2 inhibits *Shh* and *Fgf8* expression in cephalic explants

Because we observed a loss of *Fgf8* and *Shh* expression in

Table 4. Effects of recombinant BMP2 on rostral gene expression

		Explant type	Bead type	Marker	Change			n
					Increase	None	Decrease	
A	<i>Msx1</i> effects		+BMP2	<i>Msx1</i>	26	0	0	26
			+BSA	<i>Msx1</i>	0	17	0	17
			+BMP2	<i>Msx1</i> *	9	0	0	9
			+BSA	<i>Msx1</i>	0	6	0	6
B	<i>Fgf8</i> and <i>Shh</i> effects		+BMP2	<i>Fgf8</i>	0	2	28 (93%)	30
				<i>Shh</i>	0	17	13 (43%)	
			+BSA	<i>Fgf8</i>	0	18	1 (5%)	19
				<i>Shh</i>	0	19	0	
			+BMP2	<i>Fgf8</i>	0	14	10 (42%)	24
				<i>Shh</i>	0	1	23 (96%)	
			+BSA	<i>Fgf8</i>	0	11	0	11
				<i>Shh</i>	0	11	0	
C	<i>Msx1</i> effects		+BMP2 (10 µg/ml)	<i>Msx1</i>	16+, 1++	0	0	17
			+BMP2 (0.1 µg/ml)	<i>Msx1</i>	1+	6	0	7
			+BMP2 (10 µg/ml)	<i>Msx1</i>	16++	0	0	16
			+BMP2 (0.1 µg/ml)	<i>Msx1</i>	2+, 7++	0	0	9

\*Induction excluded from some rostral midline regions.  
Explants were cultured for 6 hours.

affected *Chrd*<sup>-/-</sup>;*Nog*<sup>+/-</sup> embryos, we tested whether increased BMP could elicit the same responses in wild-type explants (Table 4, part B). In type 1 explants, we observed suppression of *Fgf8* expression in nearly all cases (93%) after 6 hours of culture using BMP2 at a concentration of 10 µg/ml (Fig. 6E). Additionally, rostral domains of *Shh* expression were reduced in ~43% of explants. To determine whether this was due to greater sensitivity of the ANR or to bead placement, we used type 2 explants. In these, rostral *Shh* was repressed 96% of the time. *Fgf8* expression was significantly reduced but not completely repressed in 42% of explants (Fig. 6F). This demonstrates that *Shh* may be repressed by BMP2 in some domains without coincident *Msx1* induction. Together, these data demonstrate that effects of BMP2 on cultured cephalic explants reproduces changes in gene expression observed in affected *Chrd*<sup>-/-</sup>;*Nog*<sup>+/-</sup> embryos. Thus, antagonism of BMP activity is crucial both in the ANR and rostral ventral neural midline for *Fgf8* and *Shh* expression, respectively.

Cephalic explants deficient in *Chordin* and *Noggin* are hypersensitive to BMP

If the primary cause of the defects in *Chrd*<sup>-/-</sup>;*Nog*<sup>+/-</sup> embryos is increased BMP activity resulting from reduced BMP antagonism, explants prepared from these embryos should be more sensitive to exogenous BMP than are wild-type explants. To test this, we first compared the response of wild-type and *Chrd*<sup>-/-</sup>;*Nog*<sup>+/-</sup> explants to BMP2-soaked beads (Table 4, part C). Here, two beads were used: one between the rostral neural folds and one against the lateral neural folds of the midbrain (type 1+). Using a BMP concentration of 10 µg/ml, *Msx1* induction was consistently stronger in *Chrd*<sup>-/-</sup>;*Nog*<sup>+/-</sup> explants than in wild type (Fig. 6G). Next, we tested whether mutant explants would show *Msx1* induction at a lower BMP2 concentration than did wild-type explants. Whereas beads soaked in 10 µg/ml BMP2 strongly induced *Msx1* in wild-type explants, beads prepared in 0.1 µg/ml resulted in little or no induction (Fig. 6H). However, *Chrd*<sup>-/-</sup>;*Nog*<sup>+/-</sup> explants responded to 0.1 µg/ml BMP2-soaked beads with robust *Msx1*



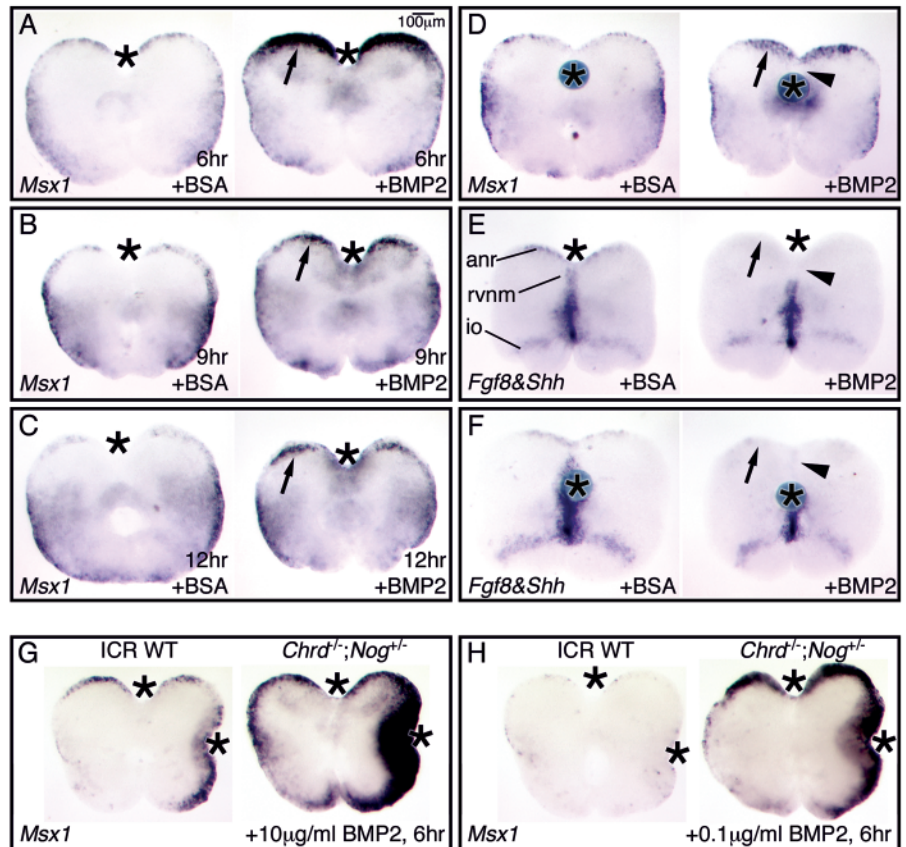
expression (Fig. 6H). Induction of *Msx1* in *Chrd*<sup>-/-</sup> explants was occasionally similar to that of *Chrd*<sup>-/-</sup>;*Nog*<sup>+/-</sup> explants, although a strong response in *Chrd*<sup>-/-</sup> explants occurred less frequently [the relative sensitivity of different *Chrd*;*Nog* genotypes to BMPs will be presented elsewhere (R. M. A. and J. K., unpublished)]. Together, these data demonstrate that *Chrd*<sup>-/-</sup>;*Nog*<sup>+/-</sup> rostral tissues are sensitized to BMP signaling, strongly supporting the premise that they are deficient in BMP antagonism.

## DISCUSSION

We have used compound mutants of *Chrd* and *Nog* null alleles to investigate the role of BMP antagonism in head development. *Chrd*<sup>-/-</sup>;*Nog*<sup>+/-</sup> mice exhibit multiple anomalies of craniofacial development, the initial defects being deficient patterning and growth of the forebrain. These problems appear to be caused by decreased activity of the PrCP and the ANR, both sites of *Chrd* and *Nog* expression. Explant culture experiments show that exogenous BMP can elicit similar gene expression changes in wild-type explants, and that *Chrd*<sup>-/-</sup>;*Nog*<sup>+/-</sup> explants are greatly sensitized to BMP. These data strongly suggest that *Chrd*;*Nog* mutants suffer from too much BMP activity in rostral tissues, and that the defects observed result from this increased BMP signaling. Collectively, the results of this study reveal a novel role for BMP antagonists in promoting the functions of rostral organizing centers during forebrain development.

### Reduced BMP antagonism in *Chrd*;*Nog* double mutants

Molecular and genetic assays used in frog, fish and fly embryos indicate that the function of both Chordin and Noggin is to antagonize BMP signaling (Furthauer et al., 1999; Holley et al., 1995; Holley et al., 1996; Piccolo et al., 1996; Schulte-Merker et al., 1997; Zimmerman et al., 1996). Thus, genetic ablation of *Chrd* and *Nog* in mice is expected to reduce BMP antagonism. We confirmed this using two methods. First, expression of *Msx1*, a positive transcriptional target of BMP signaling, is upregulated and expressed ectopically in all *Chrd*<sup>-/-</sup>;*Nog*<sup>-/-</sup> mice. This suggests increased BMP signaling in the absence of *Chrd* and *Nog*. However, ectopic *Msx1* expression was observed only in the more severely affected *Chrd*<sup>-/-</sup>;*Nog*<sup>+/-</sup> embryos, demonstrating that one wild-type allele of *Nog* is largely sufficient to control BMP signaling in the rostral head. Importantly, although *Chrd* is transcribed at low levels after gastrulation, its expression has



**Fig. 6.** Ectopic application of BMP2 to forebrain explants. (A-D) Expression of *Msx1* in cultured cephalic explants. Protein-soaked beads (represented by asterisks) were placed between rostral neural folds of five- to seven-somite wild-type cephalic explants in type 1 explants (A-C) and on the midline in type 2 explants (D). (A) BMP2 induces strong *Msx1* expression in the ANR (arrow) after 6 hours. *Msx1* is induced at large distances from the BMP2 source. (B,C) *Msx1* induction is transient and is diminished after 9 (B) and 12 (C) hours. (D) BMP2 induces *Msx1* adjacent to the caudal but not the rostral half of the bead (arrowhead). However, *Msx1* is induced in the ANR (arrow). (E,F) Expression of *Fgf8* and *Shh* (two-probe in situ hybridization) in type 1 (E) and type 2 (F) explants. (E) BMP2 suppresses the expression of *Fgf8* in the ANR (arrow) and *Shh* in the rostral ventral neural midline (arrowhead) in both explant types, whereas *Fgf8* in the isthmus organizer (io) is not affected. BSA beads had no effect in any explants. (G,H) Hypersensitivity of *Chrd*;*Nog* mutant explants to BMP signaling. BMP2-soaked beads were placed adjacent to both rostral and lateral neural folds in type 1+ explants. (G) At a concentration of 10 μg/ml, *Msx1* was induced adjacent to both beads in wild-type explants (left), but induction was more robust in *Chrd*<sup>-/-</sup>;*Nog*<sup>+/-</sup> explants (right). (H) At a concentration of 0.1 μg/ml, *Msx1* was not induced in wild-type explants (left), but was induced in *Chrd*<sup>-/-</sup>;*Nog*<sup>+/-</sup> explants (right). anr, anterior neural ridge; rvnm, rostral ventral neural midline.

great functional significance. Haploinsufficiency of *Nog* occurs only in the absence of functional *Chrd* alleles.

We also assessed the response of *Chrd*<sup>-/-</sup>;*Nog*<sup>+/-</sup> explants to exogenous BMP. We found that cephalic explants prepared from *Chrd*<sup>-/-</sup>;*Nog*<sup>+/-</sup> embryos respond to BMP2 with greater induction of *Msx1* than did wild-type explants. Moreover, *Chrd*<sup>-/-</sup>;*Nog*<sup>+/-</sup> explants exhibit robust response to BMP2 at concentrations that elicit little if any effect in wild-type explants. These results provide strong functional evidence that *Chrd*<sup>-/-</sup>;*Nog*<sup>+/-</sup> embryos possess reduced BMP antagonist activity. Complementary to these data, biochemical assays reveal that BMP signal transduction is increased in *Chrd*;*Nog* mutant embryos (R. M. A. and J. K., unpublished).

### Prechordal plate function is promoted by BMP antagonists

Midline neural deletions result from compromised function of the prechordal plate. Surgical ablation of the PrCP in mouse explants prior to four somites results in a loss of medial neural markers (Shimamura and Rubenstein, 1997), as does ablation of the PrCP in chicken (Pera and Kessel, 1997). In addition, loss of signaling molecules expressed in the PrCP, such as *Shh* in mouse (Chiang et al., 1996), results in similar neural midline defects. Affected *Chrd*<sup>-/-</sup>;*Nog*<sup>+/-</sup> mutants lack *Shh* expression in the prechordal mesendoderm, and consequently lose expression of downstream SHH targets in surrounding tissues. Thus, the resulting midline defects in *Chrd*<sup>-/-</sup>;*Nog*<sup>+/-</sup> mutants are probably due to reduction of PrCP function.

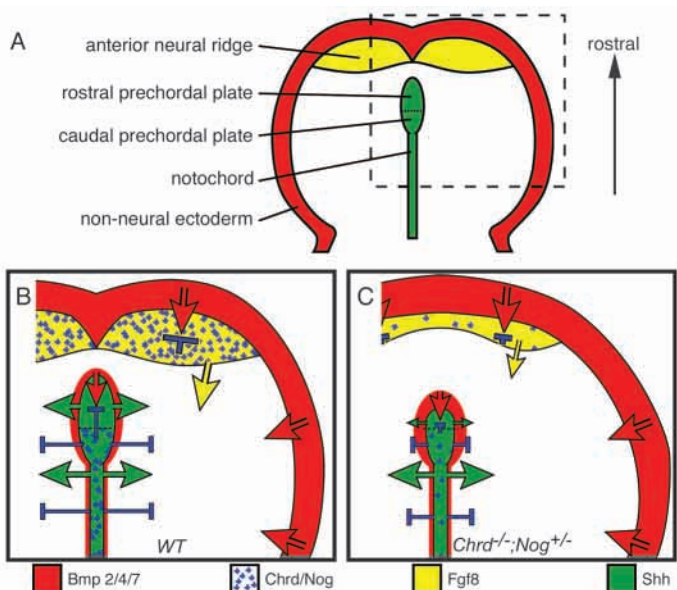
At headfold stages, *Chrd* and *Nog* are expressed in the notochord and the caudal PrCP, but not in the most rostral regions; however, both genes are expressed throughout the PrCP by the five-somite stage. This early distribution of *Chrd* and *Nog* expression reveals an initial subdivision of the PrCP into two compartments. As we have observed a clear reduction of rostral-most ventral midline tissue as early as the five-somite stage, this early compartmentalization may have functional significance. In support of this hypothesis, others have demonstrated that caudal regions of rostral midline mesendoderm are required for the maintenance of identity and function of the rostral PrCP at early somite stages (Camus et al., 2000). Thus, production of CHRD and NOG protein in the caudal compartment may be essential for the activity of the rostral PrCP.

At least three BMPs bound by CHRD and NOG are expressed adjacent to the ventral midline of the rostral neural plate in mouse. In chicken, others have shown a role for BMPs in prechordal mesoderm specification (Vesque et al., 2000). Thus, the delay in *Chrd* and *Nog* expression in rostral PrCP may provide a temporal window for this to occur. Additionally, BMP7 secretion from prechordal mesoderm may be an essential co-factor with SHH in specification of rostral ventral neural midline fates; temporal regulation of *Chrd* expression may limit this induction along the rostrocaudal axis (Dale et al., 1999). Although this suggests that loss of CHRD and NOG should promote rostral-ventral midline fates by increasing BMP7 signaling, the associated loss of rostral SHH may prevent induction of ectopic ventral fates in affected *Chrd*<sup>-/-</sup>;*Nog*<sup>+/-</sup> embryos. Alternatively, given significant differences in PrCP morphology and histology between mouse and chicken (Pera and Kessel, 1997; Sulik et al., 1994), it is possible that the PrCP may function differently in mammals and birds. Taken together, our results suggest that CHRD and NOG coordinate the location, duration and composition of BMP signaling during rostral midline development.

Our study has demonstrated that application of BMP-soaked beads mimics the abnormal gene expression of *Chrd*<sup>-/-</sup>;*Nog*<sup>+/-</sup> mutants by repressing rostral expression of *Shh* in the CNS, consistent with results from chicken (Ohkubo et al., 2002). In addition to transcriptional repression of *Shh*, BMPs can both antagonize SHH signaling and alter the response to SHH in receiving cells (Liem et al., 1995; Murtaugh et al., 1999; Watanabe et al., 1998). Thus, in *Chrd*<sup>-/-</sup>;*Nog*<sup>+/-</sup> animals, ectopic BMP signaling may affect both the expression of SHH and its signal transduction.

### Chordin and noggin in the anterior neural ridge

Rostral truncation phenotypes cannot be due to impairment of SHH signaling alone, as this type of defect never occurs in *Shh*<sup>-/-</sup> mice (Chiang et al., 1996) (R. M. A. and J. K., unpublished). However, *Chrd*<sup>-/-</sup>;*Nog*<sup>+/-</sup> mutants recapitulate rostral defects seen in some *Fgf8* mutants (Meyers et al., 1998). Furthermore, *Chrd*<sup>-/-</sup>;*Nog*<sup>+/-</sup> mutants have reduced FGF8 expression and activity in the ANR. Taken together, these data suggest that rostral neural deletions result from impairment of ANR function. Expression of *Nog* in the ANR precedes *Fgf8* expression, and by the five-somite stage, both *Chrd* and *Nog* are co-expressed with *Fgf8* in the ANR. We have shown that several BMPs are expressed in surface ectoderm adjacent to the ANR, and that BMP2 can repress *Fgf8* in the ANR in vitro. Indeed, similar transcriptional repression of *Fgf8* by BMPs has been observed in the chick ANR (Ohkubo et al., 2002), and in the first branchial arch of mouse (Stottmann et al., 2001). We therefore speculate that in addition to direct repression of the FGF8 target *Foxg1* by BMPs (Furuta et al., 1997), *Foxg1* may



**Fig. 7.** Regulation of BMP activity in rostral neural patterning. (A) Schematic representation of headfold/early somite stage neural plate with surrounding non-neural ectoderm and adjacent axial mesendoderm (after Rubenstein and Beachy, 1998). (B) In wild type, *Chrd* and *Nog* (blue crosses) are co-expressed with *Fgf8* (yellow) in the anterior neural ridge (ANR). Here, CHRD and NOG antagonize (represented by blunted blue arrow) the activity of BMPs (red arrows) secreted from the non-neural ectoderm abutting the neural plate. This promotes expression of *Fgf8*, and its function (yellow arrow). *Chrd* and *Nog* are also co-expressed with *Shh* (green) in the caudal prechordal plate (PrCP) and notochord. Here, CHRD and NOG antagonize BMPs expressed in axial mesendoderm and adjacent paraxial mesoderm, permitting SHH signaling from the rostral PrCP (green arrows). (C) In affected *Chrd*<sup>-/-</sup>;*Nog*<sup>+/-</sup> mutants, BMP antagonist expression is reduced in the ANR and the PrCP (fewer blue crosses), and thus, BMP antagonism is reduced (smaller blunted arrows). In turn, expression of *Fgf8* is repressed by BMPs in the ANR, reducing its activity (smaller yellow arrow) in adjacent tissues. Similarly, BMPs repress expression of *Shh* in the rostral PrCP, reducing its activity in surrounding tissues (smaller green arrows). In combination, these defects result in diminished growth and incorrect patterning of the rostral neural plate.



be reduced indirectly by repression of *Fgf8*. Our results suggest that CHRD and NOG may preserve endogenous expression of FGF8 in the ANR.

### Multiple roles for chordin and noggin in patterning the rostral neural plate

Our data provide evidence for two distinct roles for *Chrd* and *Nog* in patterning the rostral neural plate (Fig. 7A,B). First, CHRD and NOG secreted from the notochord and caudal PrCP antagonize the activity of BMPs expressed in the midline mesendoderm and adjacent mesodermal domains. This protects and promotes the functions of SHH and the rostral PrCP in defining the rostral neural midline. Second, CHRD and NOG secreted from the ANR antagonize BMPs that are secreted from adjacent non-neural ectoderm, and thus prevent the transcriptional repression of *Fgf8*. In the affected mutant embryos, reduced CHRD and NOG lead to lower BMP antagonism and thus increased BMP signaling; this in turn results in reduced SHH signaling from the rostral PrCP and FGF8 signaling from the ANR (Fig. 7C).

BMPs are reported to have proliferative, anti-proliferative and pro-apoptotic effects upon neural tissue (Furuta et al., 1997; Mabie et al., 1999; Mehler et al., 1997; Trousse et al., 2001). Our data support a role for CHRD and NOG in permitting proliferation during neurulation, and later in preventing apoptosis in the neural tube. At the eight- to 10-somite stage, cell proliferation in rostral neural ectoderm is decreased, while apoptosis is slightly increased. By 20–25 somites, proliferation in this tissue has essentially normalized, while apoptosis is substantially increased. We therefore suggest that the dramatic malformations in the forebrain of *Chrd*<sup>-/-</sup>;*Nog*<sup>+/-</sup> mutants are due to a combination of apoptosis-promoting and anti-proliferative activities of BMPs, together with the loss of trophic factors such as FGF8 and SHH.

### Variability and penetrance of craniofacial defects

The mutant phenotypes of *Chrd*<sup>-/-</sup>;*Nog*<sup>+/-</sup> animals showed low penetrance and wide variability. We suggest two explanations that may account for these phenomena. First, variability could result from unlinked modifier alleles that confer sensitivity to increased BMP signaling. Potential modifiers include other BMP antagonists, such as cerberus, gremlin, Dan (*Nb11*; *Parn* – Mouse Genome Informatics) and twisted gastrulation (Hsu et al., 1998; Pearce et al., 1999; Piccolo et al., 1999; Scott et al., 2001). If this were the case, the penetrance and expressivity of phenotypes in *Chrd*<sup>-/-</sup>;*Nog*<sup>+/-</sup> should depend strongly on genetic background. However, we observed that penetrance was low with wide phenotypic variability, even in a defined genetic background.

Alternatively, there may be natural stochastic variation in levels of BMP or BMP antagonist levels. We suggest that this variation does not approach upper or lower critical thresholds unless the balance between BMPs and antagonists is disrupted, as in *Chrd*;*Nog* mutants. Our studies with *Chrd*<sup>-/-</sup>;*Nog*<sup>+/-</sup> cephalic explants would seem to support this idea. At a given dose of BMP2 we saw variable increases in *Msx1* expression in explants of identical genotype. Consistent with this idea, mutants of several BMP signaling components have variable defects, including BMP2, BMP4, BMP7, and SMAD5 and SMAD6 (Chang et al., 1999; Dudley et al.,

1995; Dunn et al., 1997; Galvin et al., 2000; Winnier et al., 1995; Zhang and Bradley, 1996). This intrinsic variability in BMP signaling levels could normally be controlled by the multiple regulatory feedback loops that control BMP signaling. These include autoregulation of BMP expression levels (Ghosh-Choudhury et al., 2001; Vainio et al., 1993), as well as positive regulation by BMPs of *Chrd* and *Nog* transcription (Stottmann et al., 2001) and inhibitory SMAD expression (Afrakhte et al., 1998; Imamura et al., 1997; Nakao et al., 1997; Takase et al., 1998). Thus, regulatory mechanisms in *Chrd*;*Nog* mutants might include reduction of BMP expression and compensatory antagonism by other BMP antagonists and inhibitory SMADs.

### BMP signaling and human holoprosencephaly

The spectrum of phenotypes in *Chrd*<sup>-/-</sup>;*Nog*<sup>+/-</sup> mutants mirrors the range of defects observed in human holoprosencephaly. Furthermore, human HPE is frequently associated with micrognathia, agnathia and pituitary dysgenesis, as in affected *Chrd*<sup>-/-</sup>;*Nog*<sup>+/-</sup> mutants. HPE is common in man, occurring in as many as one out of 250 conceptuses (reviewed by Ming and Muenke, 1998). The frequency of sporadic HPE in wild-type mouse conceptuses is apparently much lower, in that we have never seen HPE in thousands of outbred embryos and fetuses examined in our laboratory (R. M. A., A. R. L., R. W. S. and J. K., unpublished). This may imply that humans are more sensitive to environmental or genetic factors that promote HPE. Consistent with this possibility, human *SHH* heterozygotes can display a partially penetrant range of HPE phenotypes, while mouse *Shh* heterozygotes do not display HPE (Chiang et al., 1996; Ming and Muenke, 1998). Overall, the variability, penetrance, and restricted location of phenotypes suggest that *Chrd*;*Nog* mutant mice reproduce many aspects of the human holoprosencephaly syndrome.

Although no BMP antagonists or BMP pathway components correspond to known HPE loci, many genes involved in human holoprosencephaly remain unidentified (Roessler and Muenke, 2001). Furthermore, it is possible that mutations in *CHRD* or *NOG* modify one or more of the known loci. Consistent with our data, other evidence suggests that BMP signaling pathways may be involved in the pathogenesis of HPE. Addition of BMP proteins to the chick forebrain leads to reduced SHH and FGF8 expression as well as midline and anterior deletions (Golden et al., 1999; Ohkubo et al., 2002). Our genetic and embryological manipulations of mouse *Chrd*<sup>-/-</sup>;*Nog*<sup>+/-</sup> mutants lead us to propose that insufficient BMP antagonism may underlie some human HPE by decreasing the activity of rostral organizing centers.

We thank our laboratory colleagues, M. Kirby, E. Meyers and J. Rubenstein for helpful discussions and critical reading of the manuscript, and J. Rubenstein for sharing unpublished results. S. May helped with initial characterization of mutant phenotypes. A. McMahon and R. Harland kindly provided noggin mutant mice. Probes were generously provided by R. Beddington, A. Joyner, G. Martin, P. Mitchell, J. Rossant, P. Gruss and J. Rubenstein. Recombinant BMPs were provided by Genetics Institute (Cambridge, MA). R. M. A. and R. W. S. were supported in part by a Cell and Molecular Biology NIH training grant to Duke University. This work was funded by awards to J. K. from NIDCR (R01DE13674) and the Whitehead Foundation, and to D. B. from the Victor Goodhill endowment.



## REFERENCES

- Afrakhte, M., Moren, A., Jossan, S., Itoh, S., Sampath, K., Westermarck, B., Heldin, C. H., Heldin, N. E. and ten Dijke, P. (1998). Induction of inhibitory Smad6 and Smad7 mRNA by TGF-beta family members. *Biochem. Biophys. Res. Commun.* **249**, 505-511.
- Ang, S. L. and Rossant, J. (1994). HNF-3 beta is essential for node and notochord formation in mouse development. *Cell* **78**, 561-574.
- Ashe, H. L. and Levine, M. (1999). Local inhibition and long-range enhancement of Dpp signal transduction by Sog. *Nature* **398**, 427-431.
- Bachiller, D., Klingensmith, J., Kemp, C., Belo, J. A., Anderson, R. M., May, S. R., McMahon, J. A., McMahon, A. P., Harland, R. M., Rossant, J. et al. (2000). The organizer factors Chordin and Noggin are required for mouse forebrain development. *Nature* **403**, 658-661.
- Barlow, A. J. and Francis-West, P. H. (1997). Ectopic application of recombinant BMP-2 and BMP-4 can change patterning of developing chick facial primordia. *Development* **124**, 391-398.
- Belo, J. A., Bouwmeester, T., Leyns, L., Kertesz, N., Gallo, M., Follettie, M. and de Robertis, E. M. (1997). Cerberus-like is a secreted factor with neutralizing activity expressed in the anterior primitive endoderm of the mouse gastrula. *Mech. Dev.* **68**, 45-57.
- Belo, J. A., Leyns, L., Yamada, G. and de Robertis, E. M. (1998). The prechordal midline of the chondrocranium is defective in Goosecoid-1 mouse mutants. *Mech. Dev.* **72**, 15-25.
- Brunet, L. J., McMahon, J. A., McMahon, A. P. and Harland, R. M. (1998). Noggin, cartilage morphogenesis, and joint formation in the mammalian skeleton. *Science* **280**, 1455-1457.
- Camus, A., Davidson, B. P., Billiards, S., Khoo, P., Rivera-Perez, J. A., Wakamiya, M., Behringer, R. R. and Tam, P. P. (2000). The morphogenetic role of midline mesendoderm and ectoderm in the development of the forebrain and the midbrain of the mouse embryo. *Development* **127**, 1799-1813.
- Chang, H., Huylebroeck, D., Verschueren, K., Guo, Q., Matzuk, M. M. and Zwijsen, A. (1999). Smad5 knockout mice die at mid-gestation due to multiple embryonic and extraembryonic defects. *Development* **126**, 1631-1642.
- Chiang, C., Litington, Y., Lee, E., Yong, K. E., Corden, J. L., Westphal, H. and Beachy, P. A. (1996). Cyclopia and defective axial patterning in mice lacking Sonic hedgehog gene function. *Nature* **383**, 407-413.
- Conlon, R. A., Reaume, A. G. and Rossant, J. (1995). Notch1 is required for the coordinate segmentation of somites. *Development* **121**, 1533-1545.
- Crossley, P. H. and Martin, G. R. (1995). The mouse Fgf8 gene encodes a family of polypeptides and is expressed in regions that direct outgrowth and patterning in the developing embryo. *Development* **121**, 439-451.
- Dale, J. K., Vesque, C., Lints, T. J., Sampath, T. K., Furley, A., Dodd, J. and Placzek, M. (1997). Cooperation of BMP7 and SHH in the induction of forebrain ventral midline cells by prechordal mesoderm. *Cell* **90**, 257-269.
- Dale, K., Sattar, N., Heemskerk, J., Clarke, J. D., Placzek, M. and Dodd, J. (1999). Differential patterning of ventral midline cells by axial mesoderm is regulated by BMP7 and chordin. *Development* **126**, 397-408.
- Downs, K. M. and Davies, T. (1993). Staging of gastrulating mouse embryos by morphological landmarks in the dissecting microscope. *Development* **118**, 1255-1266.
- Dudley, A. T., Lyons, K. M. and Robertson, E. J. (1995). A requirement for bone morphogenetic protein-7 during development of the mammalian kidney and eye. *Genes Dev.* **9**, 2795-2807.
- Dunn, N. R., Winnier, G. E., Hargett, L. K., Schrick, J. J., Fogo, A. B. and Hogan, B. L. (1997). Haploinsufficient phenotypes in Bmp4 heterozygous null mice and modification by mutations in Gli3 and Alx4. *Dev. Biol.* **188**, 235-247.
- Feledy, J. A., Beanan, M. J., Sandoval, J. J., Goodrich, J. S., Lim, J. H., Matsuo-Takasaki, M., Sato, S. M. and Sargent, T. D. (1999). Inhibitory patterning of the anterior neural plate in Xenopus by homeodomain factors Dlx3 and Msx1. *Dev. Biol.* **212**, 455-464.
- Furthauer, M., Thisse, B. and Thisse, C. (1999). Three different noggin genes antagonize the activity of bone morphogenetic proteins in the zebrafish embryo. *Dev. Biol.* **214**, 181-196.
- Furuta, Y., Piston, D. W. and Hogan, B. L. (1997). Bone morphogenetic proteins (BMPs) as regulators of dorsal forebrain development. *Development* **124**, 2203-2212.
- Galvin, K. M., Donovan, M. J., Lynch, C. A., Meyer, R. I., Paul, R. J., Lorenz, J. N., Fairchild-Huntress, V., Dixon, K. L., Dunmore, J. H., Gimbrone, M. A., Jr et al. (2000). A role for smad6 in development and homeostasis of the cardiovascular system. *Nat. Genet.* **24**, 171-174.
- Ghosh-Choudhury, N., Choudhury, G. G., Harris, M. A., Wozney, J., Mundy, G. R., Abboud, S. L. and Harris, S. E. (2001). Autoregulation of mouse BMP-2 gene transcription is directed by the proximal promoter element. *Biochem. Biophys. Res. Commun.* **286**, 101-108.
- Golden, J. A., Braciclovic, A., McFadden, K. A., Beesley, J. S., Rubenstein, J. L. R. and Grinspan, J. B. (1999). Ectopic bone morphogenetic proteins 5 and 4 in the chicken forebrain lead to cyclopia and holoprosencephaly. *Proc. Natl. Acad. Sci. USA* **96**, 2439-2444.
- Graham, A., Francis-West, P., Brickell, P. and Lumsden, A. (1994). The signalling molecule BMP4 mediates apoptosis in the rhombencephalic neural crest. *Nature* **372**, 684-686.
- Graham, A., Koentges, G. and Lumsden, A. (1996). Neural crest apoptosis and the establishment of craniofacial pattern: an honorable death. *Mol. Cell. Neurosci.* **8**, 76-83.
- Hammerschmidt, M., Serbedzija, G. N. and McMahon, A. P. (1996). Genetic analysis of dorsoventral pattern formation in the zebrafish: requirement of a BMP-like ventralizing activity and its dorsal repressor. *Genes Dev.* **10**, 2452-2461.
- Hogan, B., Beddington, R., Costantini, F. and Lacy, E. (1994). *Manipulating the Mouse Embryo*. New York: Cold Spring Harbor Press.
- Holley, S. A., Jackson, P. D., Sasai, Y., Lu, B., DeRobertis, E. M., Hoffmann, F. M. and Ferguson, E. L. (1995). A conserved system for dorsal-ventral patterning in insects and vertebrates involving sog and chordin. *Nature* **376**, 249-253.
- Holley, S. A., Neul, J. L., Attisano, L., Wrana, J. L., Sasai, Y., O'Connor, M. B., DeRobertis, E. M. and Ferguson, E. L. (1996). The Xenopus dorsalizing factor noggin ventralizes Drosophila embryos by preventing DPP from activating its receptor. *Cell* **86**, 607-617.
- Houart, C., Westerfield, M. and Wilson, S. W. (1998). A small population of anterior cells patterns the forebrain during zebrafish gastrulation. *Nature* **391**, 788-792.
- Hsu, D. R., Economides, A. N., Wang, X., Eimon, P. M. and Harland, R. M. (1998). The Xenopus dorsalizing factor Gremlin identifies a novel family of secreted proteins that antagonize BMP activities. *Mol. Cell* **1**, 673-683.
- Imamura, T., Takase, M., Nishihara, A., Oeda, E., Hanai, J., Kawabata, M. and Miyazono, K. (1997). Smad6 inhibits signalling by the TGF-beta superfamily. *Nature* **389**, 622-626.
- Kaufman, M. H. (1992). *The Atlas of Mouse Development*. San Diego: Academic Press.
- Kimura, S., Hara, Y., Pineau, T., Fernandez-Salguero, P., Fox, C. H., Ward, J. M. and Gonzalez, F. J. (1996). The *Tebp* null mouse: thyroid-specific enhancer-binding protein is essential for the organogenesis of the thyroid, lung, ventral forebrain, and pituitary. *Genes Dev.* **10**, 60-69.
- Klingensmith, J., Ang, S. L., Bachiller, D. and Rossant, J. (1999). Neural induction and patterning in the mouse in the absence of the node and its derivatives. *Dev. Biol.* **216**, 535-549.
- Lee, J., Platt, K. A., Censullo, P. and Ruiz i Altaba, A. (1997). Gli1 is a target of Sonic hedgehog that induces ventral neural tube development. *Development* **124**, 2537-2552.
- Liem, K. F., Jr, Tremml, G., Roelink, H. and Jessell, T. M. (1995). Dorsal differentiation of neural plate cells induced by BMP-mediated signals from epidermal ectoderm. *Cell* **82**, 969-979.
- Mabie, P. C., Mehler, M. F. and Kessler, J. A. (1999). Multiple roles of bone morphogenetic protein signaling in the regulation of cortical cell number and phenotype. *J. Neurosci.* **19**, 7077-7088.
- Marazzi, G., Wang, Y. and Sassoon, D. (1997). Msx2 is a transcriptional regulator in the BMP4-mediated programmed cell death pathway. *Dev. Biol.* **186**, 127-138.
- Marigo, V. and Tabin, C. J. (1996). Regulation of patched by sonic hedgehog in the developing neural tube. *Proc. Natl. Acad. Sci. USA* **93**, 9346-9351.
- McLeod, M. J. (1980). Differential staining of cartilage and bone in whole mouse fetuses by alcian blue and alizarin red S. *Teratology* **22**, 299-301.
- McMahon, J. A., Takada, S., Zimmerman, L. B., Fan, C. M., Harland, R. M. and McMahon, A. P. (1998). Noggin-mediated antagonism of BMP signaling is required for growth and patterning of the neural tube and somite. *Genes Dev.* **12**, 1438-1452.
- Mehler, M. F., Mabie, P. C., Zhang, D. and Kessler, J. A. (1997). Bone morphogenetic proteins in the nervous system. *Trends Neurosci.* **20**, 309-317.
- Meyers, E. N., Lewandoski, M. and Martin, G. R. (1998). An Fgf8 mutant allelic series generated by Cre- and Flp-mediated recombination. *Nat. Genet.* **18**, 136-141.

- Ming, J. E. and Muenke, M. (1998). Holoprosencephaly: from Homer to Hedgehog. *Clin. Genet.* **53**, 155-163.
- Murtaugh, L. C., Chyung, J. H. and Lassar, A. B. (1999). Sonic hedgehog promotes chondrogenesis by altering the cellular response to BMP signaling. *Genes Dev.* **13**, 225-237.
- Nakao, A., Afrakhte, M., Moren, A., Nakayama, T., Christian, J. L., Heuchel, R., Itoh, S., Kawabata, M., Heldin, N. E., Heldin, C. H. et al. (1997). Identification of Smad7, a TGF $\beta$ -inducible antagonist of TGF $\beta$  signalling. *Nature* **389**, 631-635.
- Ohkubo, Y., Chiang, C. and Rubenstein, J. L. (2002). Coordinate regulation and synergistic actions of BMP4, SHH and FGF8 in the rostral prosencephalon regulate morphogenesis of the telencephalic and optic vesicles. *Neuroscience* **111**, 1-17.
- Pearce, J. J., Penny, G. and Rossant, J. (1999). A mouse cerberus/Dan-related gene family. *Dev. Biol.* **209**, 98-110.
- Pera, E. M. and Kessel, M. (1997). Patterning of the chick forebrain anlage by the prechordal plate. *Development* **124**, 4153-4162.
- Piccolo, S., Sasai, Y., Lu, B. and de Robertis, E. M. (1996). Dorsoventral patterning in *Xenopus*: inhibition of ventral signals by direct binding of chordin to BMP-4. *Cell* **86**, 589-598.
- Piccolo, S., Agius, E., Lu, B., Goodman, S., Dale, L. and de Robertis, E. M. (1997). Cleavage of Chordin by Xoloid metalloprotease suggests a role for proteolytic processing in the regulation of Spemann organizer activity. *Cell* **91**, 407-416.
- Piccolo, S., Agius, E., Leyns, L., Bhattacharyya, S., Grunz, H., Bouwmeester, T. and de Robertis, E. M. (1999). The head inducer Cerberus is a multifunctional antagonist of Nodal, BMP and Wnt signals. *Nature* **397**, 707-710.
- Roessler, E., Belloni, E., Gaudenz, K., Jay, P., Berta, P., Scherer, S. W., Tsui, L. C. and Muenke, M. (1996). Mutations in the human Sonic Hedgehog gene cause holoprosencephaly. *Nat. Genet.* **14**, 357-360.
- Roessler, E. and Muenke, M. (2001). Midline and laterality defects: left and right meet in the middle. *BioEssays* **23**, 888-900.
- Rubenstein, J. L. and Beachy, P. A. (1998). Patterning of the embryonic forebrain. *Curr. Opin. Neurobiol.* **8**, 18-26.
- Sasai, Y. and de Robertis, E. M. (1997). Ectodermal patterning in vertebrate embryos. *Dev. Biol.* **182**, 5-20.
- Saxen, L. (1989). Neural Induction. *Int. J. Dev. Biol.* **33**, 21-48.
- Schier, A. F., Neuhauss, S. C., Helde, K. A., Talbot, W. S. and Driever, W. (1997). The one-eyed pinhead gene functions in mesoderm and endoderm formation in zebrafish and interacts with *no tail*. *Development* **124**, 327-342.
- Schulte-Merker, S., Lee, K. J., McMahon, A. P. and Hammerschmidt, M. (1997). The zebrafish organizer requires chordin [letter]. *Nature* **387**, 862-863.
- Scott, I. C., Blitz, I. L., Pappano, W. N., Maas, S. A., Cho, K. W. and Greenspan, D. S. (2001). Homologues of Twisted gastrulation are extracellular cofactors in antagonism of BMP signalling. *Nature* **410**, 475-478.
- Scott, I. C., Steiglitz, B. M., Clark, T. G., Pappano, W. N. and Greenspan, D. S. (2000). Spatiotemporal expression patterns of mammalian chordin during postgastrulation embryogenesis and in postnatal brain. *Dev. Dyn.* **217**, 449-456.
- Shimamura, K. and Rubenstein, J. L. R. (1997). Inductive interactions direct early regionalization of the mouse forebrain. *Development* **124**, 2709-2718.
- Stottmann, R. W., Anderson, R. M. and Klingensmith, J. (2001). The BMP antagonists Chordin and Noggin have essential but redundant roles in mouse mandibular outgrowth. *Dev. Biol.* **240**, 457-473.
- Sulik, K., Dehart, D. B., Iangaki, T., Carson, J. L., Vrablic, T., Gesteland, K. and Schoenwolf, G. C. (1994). Morphogenesis of the murine node and notochordal plate. *Dev. Dyn.* **201**, 260-278.
- Takase, M., Imamura, T., Sampath, T. K., Takeda, K., Ichijo, H., Miyazono, K. and Kawabata, M. (1998). Induction of Smad6 mRNA by bone morphogenetic proteins. *Biochem. Biophys. Res. Commun.* **244**, 26-29.
- Takuma, N., Sheng, H. Z., Furuta, Y., Ward, J. M., Sharma, K., Hogan, B. L., Pfaff, S. L., Westphal, H., Kimura, S. and Mahon, K. A. (1998). Formation of Rathke's pouch requires dual induction from the diencephalon. *Development* **125**, 4835-4840.
- Trousse, F., Esteve, P. and Bovolenta, P. (2001). Bmp4 mediates apoptotic cell death in the developing chick eye. *J. Neurosci.* **21**, 1292-1301.
- Trumpp, A., Depew, M. J., Rubenstein, J. L., Bishop, J. M. and Martin, G. R. (1999). Cre-mediated gene inactivation demonstrates that FGF8 is required for cell survival and patterning of the first branchial arch. *Genes Dev.* **13**, 3136-3148.
- Vainio, S., Karavanova, I., Jowett, A. and Thesleff, I. (1993). Identification of BMP-4 as a signal mediating secondary induction between epithelial and mesenchymal tissues during early tooth development. *Cell* **75**, 45-58.
- Vesque, C., Ellis, S., Lee, A., Szabo, M., Thomas, P., Beddington, R. and Placzek, M. (2000). Development of chick axial mesoderm: specification of prechordal mesoderm by anterior endoderm-derived TGF $\beta$  family signalling. *Development* **127**, 2795-2809.
- Watanabe, Y., Duprez, D., Monsoro-Burq, A. H., Vincent, C. and le Douarin, N. M. (1998). Two domains in vertebral development: antagonistic regulation by SHH and BMP4 proteins. *Development* **125**, 2631-2639.
- Winnier, G., Blessing, M., Labosky, P. A. and Hogan, B. L. M. (1995). Bone morphogenetic protein-4 is required for mesoderm formation and patterning in the mouse. *Genes Dev.* **9**, 2105-2116.
- Zhang, H. and Bradley, A. (1996). Mice deficient for BMP2 are nonviable and have defects in amnion/chorion and cardiac development. *Development* **122**, 2977-2986.
- Zimmerman, L. B., de Jesus-Escobar, J. M. and Harland, R. M. (1996). The Spemann organizer signal noggin binds and inactivates bone morphogenetic protein-4. *Cell* **86**, 599-606.